Physics of Magnetic Stars, 2007, pp. 315–324

Propagation of pulsation waves in roAp atmospheres

M. Sachkov[1], T. Ryabchikova[1,2], O. Kochukhov[3], D. Lyashko[4]

[1] Institute of Astronomy, Russian Academy of Sciences, Pyatnitskaya 48, 119017 Moscow, Russia
[2] Department of Astronomy, University of Vienna, Türkenschanzstrasse 17, A-1180 Wien, Austria
[3] Department of Astronomy and Space Physics, Uppsala University Box 515, SE-751 20 Uppsala, Sweden
[4] Tavrian National University, Yaltinskaya 4, 330000 Simferopol, Ukraine

Abstract.

We present a detailed analysis of the vertical cross-section of the roAp pulsation modes in eight rapidly oscillating (roAp) stars basing on spectroscopic time-series observations. We propose to use the phase-amplitude diagram as the first step in the interpretation of roAp pulsational observations. Such an approach has an advantage of being suitable to compare the behaviour of different elements, which is impossible for studies of phase / amplitude dependence on line intensity.

Although the overall pulsational behaviour of roAp stars is not identical, we found certain common features. The phase shifts of the RV curves are arranged in the following sequence: the lowest RV amplitudes are detected in the layers of Eu II (and Fe in 33 Lib) line formation, then pulsations go through the layers where the Hαcore, Nd and Pr lines are formed, the RV amplitude reaches a maximum and after that, in most stars, shows a decrease of the amplitude. The phases of RV curves of the first ions are always followed by the second ones. The largest phase shifts are detected in the Tb III and Th III lines. A pulsational variability of the Th III lines has been detected and studied for the first time. In the atmospheres of roAp stars with the pulsation frequency below the cut-off frequency, pulsations have a standing wave character in the deeper layers and then behave like a running wave in the outer layers.

Key words: stars: atmospheres – stars: chemically peculiar – stars: magnetic fields – stars: oscillations

1 Introduction

More than 30 cool Ap stars exhibit high-overtone, low-degree, non-radial p-mode pulsations with periods in the range of 6–21 minutes (Kurtz & Martinez 2000), with their observed pulsation amplitudes modulated according to the visible magnetic field structure. These *rapidly oscillating Ap* (roAp) stars are key objects for asteroseismology, which presently is the most powerful tool for testing theories of stellar structure and evolution. The van Hoof effect (van Hoof & Struve 1953) – phase lag between radial velocity curves of lines of different elements and ions – is one of the most interesting phenomenon in roAp stars. It is interpreted as the consequence of the wave propagation through the atmosphere: starting from the inner part of the star, the wave encounters first the deepest layers and then the outermost ones during its propagation. The time it takes to cover this distance produces the observed phase lag. This effect yields a unique possibility for the vertical atmospheric structure analysis. At the same time, reconstruction of the roAp vertical at-

mospheric structure encounters many difficulties: one has to take into account vertical stratification effects, construct a self-consistent stratified atmospheric model and then estimate the influence of the surface element distribution and of the magnetic field.

To constrain the vertical cross-section of an Ap-star atmosphere, we need to know the formation depth of spectral lines. This requires a stratification analysis of stellar atmosphere with NLTE effects taken into account. Up to now such an analysis has been made for one star only, HD 24712 (Sachkov et al. 2006). We analyzed the Hα core, Nd, Pr, Ca, Sr, Ba and Fe lines (see bottom panel of Fig. 6). The abundance distribution of the different elements allows us to calculate the formation depth of individual spectral lines and then to construct a distribution of pulsation amplitudes and phases with optical depth. It was shown that a non-adiabatic model for axisymmetric non-radial pulsations in the presence of a dipole magnetic field (Saio 2005) roughly explains amplitude and phase distribution up to $\log \tau_{5000} = -4$: amplitude and phase increase towards the outer layers (Sachkov et al. 2006), which gives an evidence for pulsation wave propagating through the stellar atmosphere. In this way, the later in time the pulsation wave reaches its maximum, the higher in the atmosphere a chemical element is concentrated.

An agreement of the observed amplitude and phase distribution with the theoretical predictions encourages us to use pure observables — amplitude-phase diagrams — for an analysis of the vertical structure of p-modes and for a study of the pulsation wave propagation. Therefore, the aim of this analysis is to derive from observations a complete picture of the depth-dependence of amplitudes and phases of propagating waves without estimating line depth formation itself and then to correlate the resulting vertical mode cross-section with other pulsational characteristics. For our analysis we chose a sample of slowly rotating roAp stars.

A full paper describing our investigation has been submitted to Astronomy and Astrophysics.

2 Observations and data reduction

The ESO Archive facility was used to search for and retrieve science exposures and the respective calibration frames. The main observational dataset analyzed in our study consists of observations of 6 roAp stars obtained with the UVES instrument at the ESO VLT between October 8, 2003 and March 12, 2004 in the context of the observing program 072.D-0138.

The red 600 nm UVES dataset was complemented by the observations of HD 24712 obtained on November 11, 2004 in the DDT program 274.D-5011. A detailed description of the acquisition and reduction of these data was given by Ryabchikova et al. (2007a).

For the roAp star HD 201601 (γ Equ) we analysed 70 spectra obtained on 19 August, 2003 with the NES spectrograph attached to the 6-m telescope of the Special Astrophysical Observatory of the Russian Academy of Sciences. These échelle spectra cover a region of 4250–6000 Å and have a typical S/N of ≈ 80. The data were recorded by Kochukhov et al. (2004), who searched for rapid magnetic field variability in γ Equ. We refer readers to the latter paper for the details on the acquisition and reduction of the time-series observations at the SAO 6-m telescope.

A detailed description of the observations made for each target is presented in Table 1.

All UVES spectra were reduced and normalized to the continuum level with a routine specially developed by one of us (DL) for a fast reduction of spectroscopic time-series observations. A special modification of Vienna automatic pipeline for échelle spectra processing (Tsymbal et al. 2003) was developed. All bias and flat field images were median averaged before calibration. The scattered light was subtracted by using the 2-D background approximation. For cleaning cosmic ray hits we used an algorithm which compares the direct and reversed spectral profiles. To determine the boundaries of échelle orders, the code used a special template for each order position in each row across the dispersion axes. The shift of the row spectra relative to the template was derived by a cross-correlation technique. The wavelength calibration was based on a single ThAr exposure

recorded immediately after each stellar time-series. The calibration was performed by the usual 2-D approximation of the dispersion surface. An internal accuracy of 30–40 $\mathrm{m\,s^{-1}}$ was achieved by using several hundred ThAr lines in all échelle orders. The final step of continuum normalization and merging of échelle orders was carried out by transformation of the flat field blaze function to the response function in each order.

Table 1: Log of time-series observations of roAp stars. The columns give the star's name, heliocentric Julian dates for the middle time of spectroscopic monitoring, number of observations, exposure and overhead times, peak signal-to-noise ratio of individual spectra and information about the telescope and instrument with which the data were obtained.

Star	HJD (2450000+)	Number of exposures	Exposure time (s)	Overhead time (s)	Peak S/N	Telescope/Instrument (observing mode)
HD 12932	2921.66383	69	80	25	90	VLT/UVES (600 nm)
HD 19918	2921.56756	69	80	25	100	VLT/UVES (600 nm)
HD 24712	3321.70077	92	50	22	300	VLT/UVES (390+580 nm)
HD 101065	3071.71895	111	40	25	180	VLT/UVES (600 nm)
HD 122970	3069.75168	111	40	25	160	VLT/UVES (600 nm)
HD 134214	3070.81710	111	40	25	260	VLT/UVES (600 nm)
HD 137949	3071.80455	111	40	25	350	VLT/UVES (600 nm)
HD 201601	2871.51383	70	80	42	80	SAO 6-m/NES (425–600 nm)

The global continuum normalization was improved by iterative fit of a smoothing spline function to the high points in the average spectrum of each roAp star. With this procedure we have corrected an underestimate of the continuum level, unavoidable in the analysis of small spectral regions of the crowded spectra of cool Ap stars. A correct determination of the absolute continuum level is important for retrieving unbiased amplitudes of radial velocity variability, when the centre-of-gravity method is used. In addition to the global continuum correction, spectroscopic time-series were post-processed to ensure a homogeneity in the continuum normalization of individual spectra. The extracted spectra were divided by the mean, the resulting ratio was heavily smoothed and then used to correct continua in individual spectra. Without this correction a spurious amplitude modulation of pulsation in variable spectral lines may arise because of the inconsistent continuum normalization.

Post-processing of the échelle spectra of HD 201601 was executed consistently with the procedure adopted for the main dataset.

3 Fundamental parameters of program stars

Fundamental parameters of the program stars are given in Table 2. For five stars effective temperatures $T_{\rm eff}$, surface gravities $\log g$, and mean surface magnetic fields $\langle B_{\rm s}\rangle$ were taken from the literature. For the 3 remaining stars, HD 12932 HD 19918 and HD 134214, atmospheric parameters were derived using Strömgren photometric indices (Hauck & Mermilliod 1998) with the calibrations by Moon & Dworetsky (1985) and by Napiwotzki et al. (1993) implemented in the `TEMPLOGG` code (Rogers 1995). In addition, Geneva photometric indices (Burki et al. 2005)[1] with the calibration of Hauck & North (1993) were used for effective temperature determination. The colour excesses were

[1] `http://obswww.unige.ch/gcpd/ph13.html`

Table 2: Fundamental parameters of target stars.

HD number	$T_{\rm eff}$ (K)	$\log g$	$v_{\rm e}\sin i$ (km s^{-1})	$\langle B_{\rm s}\rangle$ (kG)	P (min)	Reference
12932	7620	4.15	3.5	1.7	*11.633*	this paper
19918	8110	4.34	3.0	1.6	*11.052*	this paper
24712	7250	4.30	5.6	3.1	*6.125*, 6.282	Ryabchikova et al. 1997
101065	6600	4.20	2.0	2.3	*12.171*	Cowley et al.2000
122970	6930	4.10	4.5	2.3	*11.187*	Ryabchikova et al. 2000
134214	7315	4.45	2.0	3.1	*5.690*	this paper
137949	7550	4.30	$\leq$2.0	5.0	*8.271*,4.136, 9.422	Ryabchikova et al. 2004
201601	7700	4.20	$\leq$1.0	4.1	*12.20*	Ryabchikova et al. 2002

estimated from the reddening maps by Lucke (1978). In Table 2 we present average values of the effective temperatures derived with three different calibrations. A typical dispersion is $\pm$150 K.

For all stars, but for HD 101065, rotation velocities were estimated by fitting line profiles of the magnetically insensitive Fe I 5434.5, 5576.1 lines. The magnetic spectrum synthesis code `SYNTHMAG` (Kochukhov 2007) was used in our calculations. Atomic parameters of spectral lines were extracted from the `VALD` (Kupka et al. 1999) and `DREAM` (Biémont et al. 1999) databases, supplemented with the new oscillator strengths for La II (Lawler et al. 2001), Nd II (Den Hartog et al. 2003), Nd III (Ryabchikova et al. 2006), Sm II (Lawler et al. 2006), Gd II (Den Hartog et al. 2006). We confirmed the rotation velocities derived previously for HD 24712, HD 122970, HD 137949, and HD 201601. The high spectral resolution of the present data allows us to improve the rotation velocity in HD 101065 using partially resolved Zeeman patterns in numerous lines of the rare-earth (REE) elements. The value of the magnetic field, 2.3 kG (Cowley et al. 2000), was confirmed.

4 Radial velocity measurements

To study the selective pulsational amplitudes in spectral lines of different chemical elements/ions, one has to be very careful in the choice of lines for pulsation measurements. For this purpose, we have synthesized the observed spectral region for each star with the model atmosphere parameters and magnetic field values from Table 2. Abundances for HD 24712, HD 101065, HD 122970, HD 137949, and HD 201601 were taken from the papers cited in the last column of Table 2. For the remaining three stars abundances were estimated in this paper. The radial velocities were measured with a centre-of-gravity technique. We used only unblended or minimally blended lines. In some cases where the line of interest was partially overlapping with the nearby lines, the unblended central part of the line was integrated, therefore some lines were not measured between the continuum points. This usually leads to lower pulsation amplitudes if we have strong variations of the pulsation signal across a spectral line (see γ Equ – Sachkov et al. 2004, and HD 99563 – Elkin et al. 2005). Bisector radial velocity measurements were performed for the Hα core. Two strongest Th III lines at $\lambda\lambda$ 5376.13 and 6599.48 have been measured for RV pulsational variability for the first time in the spectra of a few stars from our sample.

5 Period analysis

Although a detailed frequency analysis is not a primary goal of this paper, we repeated it here using a discrete Fourier transformation (DFT). The period corresponding to the highest amplitude value was then improved by the sine wave least-squares fitting of RV data to the pulsation period, amplitude and phase as free parameters. The sine wave was removed from the data and then Fourier

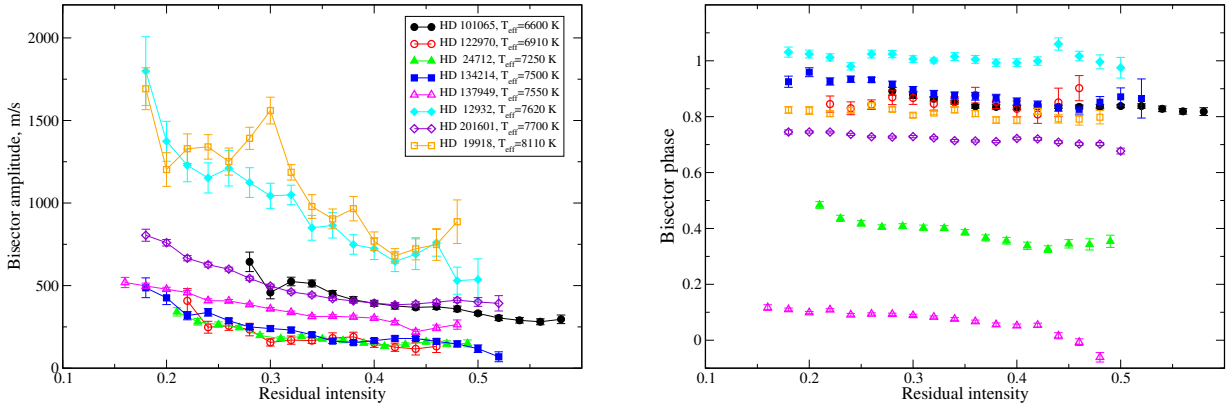

Figure 1: Bisector measurements in the Hα core of the program stars. The RV amplitudes are shown in the left panel and pulsation phases (based on the main periods from Table 2) in the right panel.

analysis was applied to the residuals. This procedure was repeated for all frequencies with a signal-to-noise ratio above 5.

For each spectral line we estimated the probability of the variation with a given period using the prescription by Horne & Baliunas (1986). For lines with the probabilities higher than 0.999 we calculated a weighted average value of the pulsation period. This value was used for subsequent determination of amplitude and phase. If a star had one dominant period, a further RV analysis was made with this period. In the cases of more than one dominant period, simultaneous fit with up to three periods was performed. RV variation was approximated by the expression:

$$\langle V \rangle = V_0(t - t_0) + \sum_{i=1}^{3} V_i \cos\{2\pi[(t - t_0)/P_i - \varphi_i]\}. \quad (1)$$

Here the first term takes into account possible drift of the spectrograph's zero point. For all stars, but for HD 24712, HJD of the first exposure of the star at a given night was chosen as a reference time t_0. For HD 24712 HJD=2453320.0 was used as a reference time. V_{ji} and φ_{ji} are amplitude and phase of the RV variability with the i-th period ($i_{max} = 3$), respectively. With the minus sign in front of φ_i a larger phase corresponds to a later time of the RV maximum. This phase agreement is natural when discussing effects of the outward propagation of pulsation waves in the atmospheres of roAp stars.

The periods participating in the RV amplitude and phase analysis are given in the seventh column of Table 2. If more than one period was used in fitting procedure, we marked by italics the period for which RV amplitudes and phases were calculated.

6 Bisector measurements in the Hα core

Fig. 1 shows bisector amplitudes (left panel) and phases (right panel) across the core of the Hα line calculated with the pulsation periods from Table 2. Where two periods or the main period and its first harmonic are resolved, simultaneous fit with two frequencies was done. In all program stars an increase of the bisector amplitude two or more times from the transition region to the deepest part of the core is observed to be in full agreement with the results obtained by Kurtz et al. (2005a). Bisector RV changes are accompanied by small phase changes. Only in three stars phase changes exceed the measurement errors. These are the stars with the shortest pulsation periods close to cut-off frequencies: HD 24712, HD 132214 and HD 137949 (33 Lib). NLTE calculations show that in the atmosphere of a normal star with $T_{\rm eff}$ between 7000 and 8000 K the Hα core is formed at

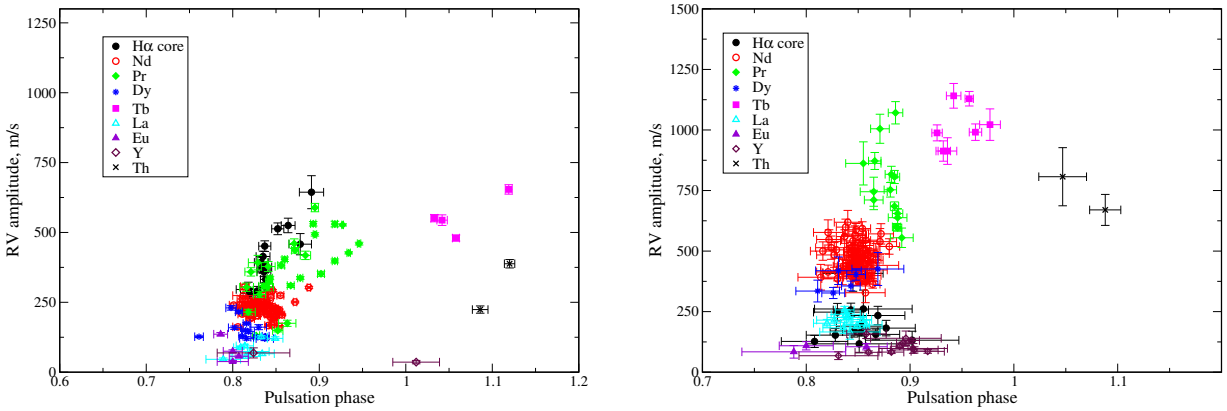

Figure 2: HD 101065 (left panel) and HD 122970 (right panel). These stars with the lowest effective temperatures show practically constant pulsation phase throughout most of the atmosphere. Phase shifts observed in the layers of Tb III and Th III line formation.

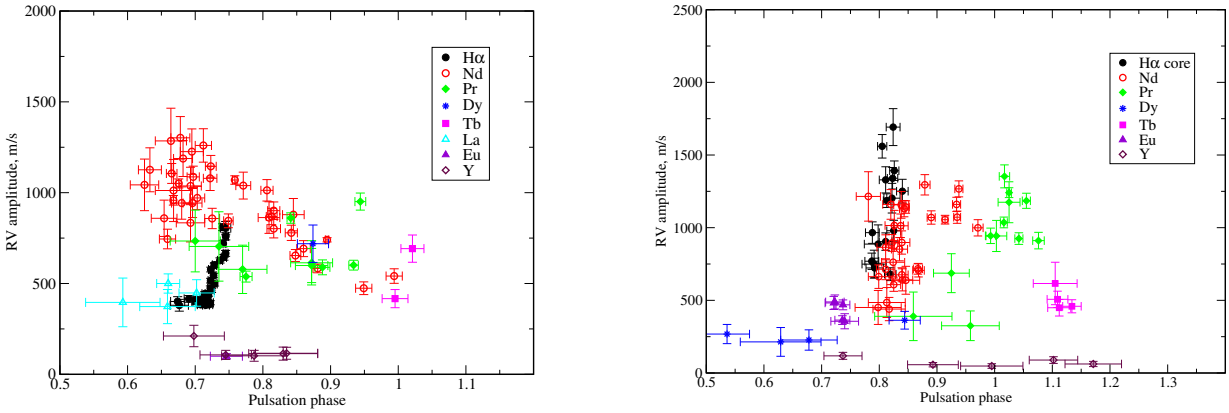

Figure 3: HD 201601 (left panel) and HD 19918 (right panel). These stars show the largest RV amplitudes. In both stars we observed first an increase of the RV amplitudes with approximately constant phases (standing wave) and after that the pulsation wave is transforming into a running one.

$-5 \lesssim \log \tau_{5000} \lesssim -2$ (Mashonkina, private communication). However, in all program stars a core-wing anomaly is present (Cowley et al. 2000), which was explained by a temperature bump below $\log \tau_{5000} = -4$ (Kochukhov et al. 2002). This change in the atmospheric structure may lead to an upward shift in formation depth of the base of the Hα core (Mashonkina, private communication).

7 Phase-amplitude diagrams

In all stars we have detected pulsational variability in the lines of rare-earth elements, which show a maximum radial velocity (RV) amplitude. Our analysis is thus based primarily on REE lines. In addition, for HD 137949 we used the pulsation signal present in Fe lines. From 14 rare-earth elements we primarily used those with the observed lines in the first and second ionization stages (Pr, Nd, Tb. Dy). We also analyzed Y II lines where the low amplitude pulsations were registered. This element is interesting by its pulsation phases: in all stars where pulsations were detected in Y II lines, pulsation phases correspond to those for Pr III lines which have the highest amplitudes.

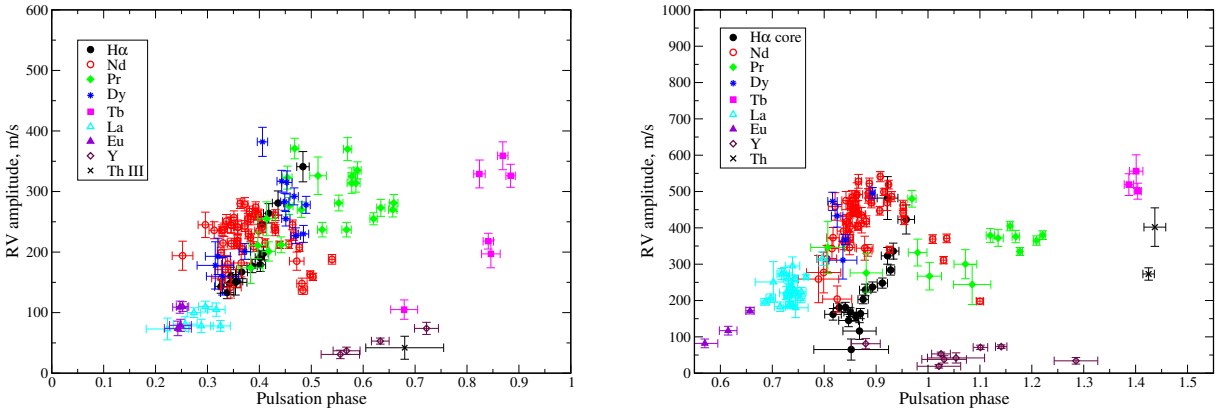

Figure 4: HD 24712 (left panel) and HD 134214 (right panel). These stars have the shortest pulsation periods close to or below the limit defined by the acoustic cut-off frequency. Phase changes for all elements are explained by a running wave through the whole atmosphere. Running waves in short-period roAp stars are predicted to exist by non-adiabatic pulsation theory (Saio, private communication).

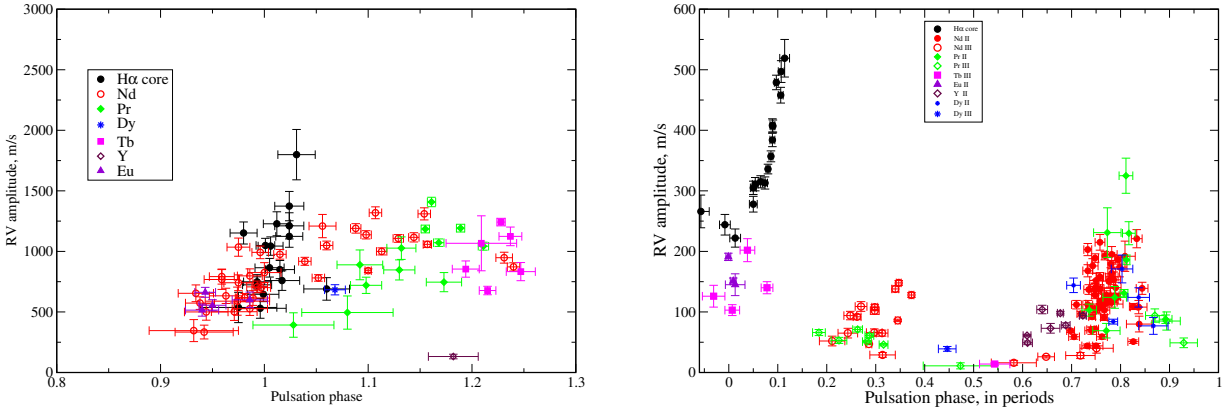

Figure 5: HD 12932 (left panel) is an example of the star with a standing wave behaviour in the layers of the Hα core formation. HD 137949 (right panel) shows the most complex pulsational behaviour among all roAp stars.

In Figures 2–5 we show phase-amplitude plots for stars in our sample.

Finally, for the first time we have found pulsations in doubly-ionized thorium lines in four coolest roAp stars of our sample: HD 101065, HD 122970, HD 24712 and HD 134214. Similar to REEs, thorium shows characteristic abundance anomaly: a 1–2 dex difference in the element abundance derived from the lines of the first and second ions. We attribute this anomaly to a strong vertical stratification similar to REEs — a layer with 4–5 dex overabundance above $\log \tau_{5000} = -4$. At present thorium is the heaviest element with this kind of stratification which shows measurable pulsation amplitudes.

Although the overall pulsational behaviour in roAp stars is different, we found certain common features. The phase shifts of the RV curves are arranged in the following sequence:
- the lowest RV amplitudes are detected in the layers where the Eu II (and Fe in 33 Lib) lines form, then they go through the layers where the $H\alpha$ core, Nd and Pr lines are formed, reach maximum and after that, show a decrease of the amplitude in most stars;
- the maximum RV of the second REE ions is always delayed relative to that of the first ones;

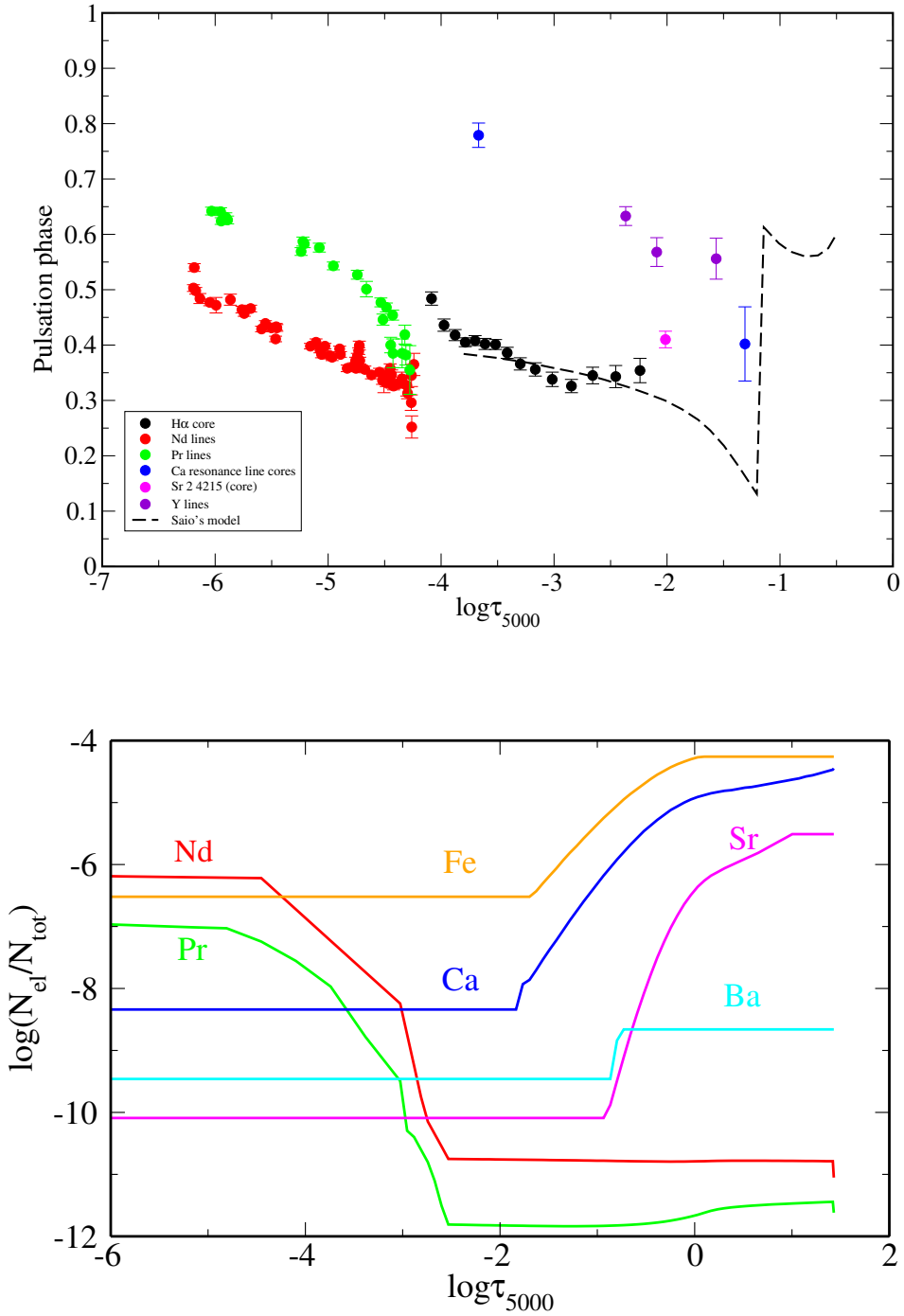

Figure 6: Upper panel: distribution of pulsation phases with optical depth in HD 24712. Dashed curve shows prediction of non-adiabatic theoretical pulsation model by Saio (private communication). Bottom panel: stratification of chemical abundances used in NLTE calculations of line formation depths for HD 24712.

- the largest phase shifts are detected in Tb III and Th III lines;
- in the atmospheres of roAp stars with the pulsation frequency below the cut-off frequency pulsations have a standing wave character in the deeper layers and then behave like a running wave in the outer layers. In three stars: HD 24712, HD 134214, which have pulsation frequency close to (or even higher than) the cut-off frequency, the pulsation wave behaves like the running one from the deeper layers;
- Y II lines show the lowest detectable RV amplitudes. However, their phases differ by ≈0.5 period from other weakly pulsating lines.

8 HD 24712

HD 24712 is the best studied star, for which an analysis of the line formation depths was performed taking into account NLTE effects and stratification. Abundance distribution of a few elements is shown in Fig. 6 (bottom panel) (see also Ryabchikova et al. 2007b). According to NLTE analysis, spectral lines of Nd and Pr are formed at nearly the same layers in the stellar atmosphere. Hence the phase shift between RV curves of individual lines of these elements (Fig. 6, upper panel) can not be explained in terms of their different vertical distribution. The difference in horizontal distribution of these elements (see Lüftinger et al., this conference) may give rise to the observed phase shifts.

Acknowledgements. Resources provided by the electronic databases (VALD, SIMBAD, NASA's ADS) are acknowledged. This work was supported by the research grants from RFBI (04-02-16788a, 06-02-16110a, 06-02-16379a), from the Swedish *Kungliga Fysiografiska Sällskapet* and *Royal Academy of Sciences* (grant No. 11630102), and from Austrian Science Fund (FWF-P17580).

References

Biémont E., Palmeri P., & Quinet P., 1999, Astrophys. Space Sci., **635**, 2691.
Burki G. et al. 2005, GENEVA photometric database, Geneva Observatory
Cowley C. R., Hubrig S., Ryabchikova T., Mathys G., Piskunov N., & Mittermayer P., 2001, Astron. Astrophys., **367**, 939
Cowley C. R., Ryabchikova T., Kupka F., Bord D. J., Mathys G., & Bidelman W. P., 2000, MNRAS, **317**, 299
Den Hartog E.A., Lawler J.E., Sneden C., & Cowan J.J., 2003, Astrophys. J. Suppl. Ser., **148**, 543
Den Hartog E.A., Lawler J.E., Sneden C., & Cowan J.J., 2006, Astrophys. J. Suppl. Ser., **167**, 292
Elkin V.G., Kurtz D.W., & Mathys G., 2005, MNRAS, **364**, 864
Hauck B., & North P., 1993, Astron. Astrophys., **269**, 403
Hauck B., & Mermilliod M., 1998, Astron. Astrophys. Suppl. Ser., **129**, 431
Horne J. H., & Baliunas S. L., 1986, Astrophys. J., **302**, 757
Kochukhov O., Bagnulo S., & Barklem P.S., 2002, Astrophys. J., **578**, L75
Kochukhov O., Ryabchikova T., Piskunov N., 2004, Astron. Astrophys., **415**, L13
Kochukhov O., & Bagnulo S., 2006a, Astron. Astrophys., **450**, 763
Kochukhov O., 2007, this proceedings
Kurtz D. W., & Martinez P., 2000, Baltic Astron., **9**, 253
Kurtz D. W., Elkin V.G., & Mathys G., 2005a, in *Element Stratification in Stars: 40 Years of Atomic Diffusion*, eds. G. Alecian, O. Richard & S. Vauclair, EAS Publ. Ser., **17**, 91
Kupka F., Piskunov N., Ryabchikova T.A., Stempels H.C., & Weiss W.W., 1999, Astron. Astrophys. Suppl. Ser., **138**, 119
Lawler J. E., Bonvallet G., & Sneden C., 2001a, ApJ, **556**, 452
Lawler J. E., Den Hartog E. A., Sneden C. & Cowan J. J., 2006, Astrophys. J. Suppl. Ser., **162**, 227
Lucke P. B., 1978, Astron. Astrophys., **64**, 367
Moon T. T., & Dworetsky M. M., 1985, Mon. Not. R. Astron. Soc., **217**, 305
Napiwotzki, R/. Schönberner, D., & Wenske, V. 1993, Astron. Astrophys., **268**, 653
Rogers N. Y., 1995, Comm. in Asteroseismology, 78

Ryabchikova T. A., Landstreet J. D., Gelbmann M. J., Bolgova G. T., Tsymbal V. V., & Weiss W. W., 1997, Astron. Astrophys., **327**, 1137
Ryabchikova T. A., Savanov I. S., Hatzes A. P., Weiss W. W., & Handler G., 2000, Astron. Astrophys., **357**, 981
Ryabchikova T., Piskunov N., Kochukhov O., Tsymbal V., Mittermayer P., & Weiss W. W., 2002, Astron. Astrophys., **384**, 545
Ryabchikova T., Nesvacil N., Weiss W. W., Kochukhov O., & Stütz Ch., 2004, Astron. Astrophys., **423**, 705
Ryabchikova T., Wade G.A., Aurière M., et al., 2005, A&A, **429**, L55
Ryabchikova T., Ryabtsev A., Kochukhov O., & Bagnulo S., 2006, Astron. Astrophys., **456**, 329
Ryabchikova T., Sachkov M., Weiss W. W., et al., 2007a, Astron. Astrophys., **462**, 1103
Ryabchikova T., Mashonkina L., Ryabtsev A., Kildiyarova R., & Khristoforova M., 2007b, Comm. in Asteroseismology, **148** (in press)
Sachkov M., Ryabchikova T., Kochukhov O., et al., 2004, in *Variable Stars in the Local Group*, eds. D.W. Kurtz & K.R. Pollard, ASP Conf. Ser., **310**, 208
Sachkov M., Ryabchikova T., Bagnulo S., et al., 2006, MemSAI, **77**, 397
Saio H., 2005, Mon. Not. R. Astron. Soc., **360**, 1022
Saio H., & Gautschy A., 2004, Mon. Not. R. Astron. Soc., **350**, 485
Savanov I. S., Malanushenko V. P., & Ryabchikova T. R., 1999, Astron. Lett., **25**, 802
Tsymbal V., Lyashko D., & Weiss W. W., 2003, in *Modelling of Stellar Atmospheres*, IAU Symp. No. 210, eds. N. Piskunov, W.W.Weiss, D.F. Gray, ASP, E49
van Hoof A., & Struve O., 1953, Publ. Astr. Soc. Pacific, **65**, 158